



ORIGINAL ARTICLE

Regulation of the PI3K/AKT/mTOR signaling pathway with synthesized bismuth oxide nanoparticles from Ginger (*Zingiber officinale*) extract: Mitigating the proliferation of colorectal cancer cells



Yaxing Zhou^a, Hai Zhang^b, Zhiyi Cheng^a, Honggang Wang^{a,*}

^a Department of Hepatobiliary Surgery, Taizhou People's Hospital, The Fifth Affiliated Hospital of Nantong University, Taizhou 225300, China

^b Department of Hepatobiliary Surgery, Affiliated Hospital of Jiangsu University, 212001, China

Received 12 October 2021; accepted 2 December 2021

Available online 9 December 2021

KEYWORDS

Bismuth nanoparticles;
Ginger extract;
Synthesis;
Characterization;
Colorectal cancer;
Signaling pathway

Abstract In order to overcome the limitations of conventional therapeutic systems in the treatment of cancer, nanoparticles (NPs) have been rapidly produced and developed as a separate treatment method for control of cancer. Synthesis of nanoparticles using plant-based materials (green synthesis), due to the easy and cost-effective synthesis, production of non-toxic, sustainable and environmentally friendly products, can be considered the most appropriate method for preparation of NPs. In this study, after synthesis of Bi₂O₃ NPs using Ginger (*Zingiber officinale*) root (rhizome) extract, the synthesized NPs were characterized and their potential application as selective anticancer agents against HCT116 colorectal cancer cells was evaluated through regulation of PI3K/AKT/mTOR signaling pathway, whereas the human kidney (HK-2) cells were used as normal cells. FTIR analysis showed a band at 673 cm⁻¹ attributed to Bi-O vibration with a fingerprint region at 1291 cm⁻¹ demonstrating the attachment of the organic molecules to the synthesized Bi₂O₃ NPs. UV-visible study showed a λ_{max} of around 268 nm, whereas XRD analysis showed eight clear peaks, demonstrating the crystalline phase of synthesized Bi₂O₃ NPs. TEM analysis showed that spherical-shaped Bi₂O₃ NPs have a size range of 20–50 nm with a mean size of around 35 nm. Finally, DLS analysis determined that Bi₂O₃ NPs have a hydrodynamic size of about 71.19 nm (PDI of 0.179) and a zeta

* Corresponding author at: No.366, Taihu Road, Hailing District, Taizhou 225300, China.

E-mail address: honggangtz@163.com (H. Wang).

Peer review under responsibility of King Saud University.



potential value of -44.39 mV, revealing the good colloidal stability of NPs. Cellular assays (MTT, LDH, flow cytometry, and RT-qPCR) showed that synthesized Bi_2O_3 NPs selectively induced anticancer effects against HCT116 colorectal cancer cells through membrane leakage, generation of ROS, induction of apoptosis via dysregulation of Bax, Bcl-2 and caspase-3 at mRNA level mediated via regulation of PI3K/AKT/mTOR signaling pathway. In conclusion, it may be suggested that the presence study could provide useful information for the potential anticancer effects mediated by synthesized Bi_2O_3 NPs in vitro, although further studies, including *in vivo* studies and clinical trials, are needed to support our findings.

© 2021 The Author(s). Published by Elsevier B.V. on behalf of King Saud University. This is an open access article under the CC BY-NC-ND license (<http://creativecommons.org/licenses/by-nc-nd/4.0/>).

1. Introduction

Nanotechnology is one of the leading common research disciplines in the world due to its efficacy and potential economic impact in health-care and industrial sectors (Coelho et al., 2012). Nanomaterials are usually introduced as particles with special structural features and sizes at a scale of 100 nm (Powers et al., 2007). Nanoparticles (NPs) can be fabricated using different routes including physical, chemical, biological and hybrid techniques (Iravani et al., 2014). Physical and chemical methods both need high-energy radiation, presence of concentrated chemical reducers, as well as stabilizing compounds that produce adverse effects (Jamkhande et al., 2019). Hence, the biosynthesis of NPs with a single-step biodegradation route that requires minimum energy to fabricate highly biocompatible and safe NPs is highly recommended (Soni et al., 2018). Plant extracts are usually used to biodegrade metal ions to form NPs. Previous reported have documented that plant metabolites such as total and reduced sugars, terpenoids, polyphenols, alkaloids, phenolic acids, and macromolecules (proteins) can play an important role in reducing metal ions and converting them into NPs, which also result in the stability of NPs after fabrication (Mittal et al., 2013; Jadoun et al., 2021).

Cancer is the uncontrolled proliferation of cells in which apoptosis is inhibited. Therefore, due to the complexity at the genetic and phenotypic levels, it requires a very complex treatment process. Colorectal cancer is one of the leading causes of death in the world and is the second leading cause of cancer in women and the third leading cause of cancer in men (Haggar et al., 2009). The pathogenesis of colorectal cancer is very complex and is influenced by various factors, some of which are related to diet and lifestyle, while others are due to genetic factors (Gingras et al., 2011).

The overexpression of multidrug resistance proteins at the surface of cancer cells, prevents the penetration and accumulation of chemotherapy drugs inside the cancer cell, which results in the development of resistance to anti-cancer drugs in tumor cells (Mullins et al., 2011; Wang et al., 2021a, 2021b). Given these problems, nanotechnology has revolutionized the selective treatment of cancer cells (Wang et al., 2020). NPs are designed to be targeted to target cells through various modifications such as changes in size, shape, physical and chemical properties (Mitchellet et al., 2021). They can selectively inhibit the proliferation of cancer cells through active or inactive targeting (Sanna et al., 2020). Ginger (*Zingiber officinale*)-derived NPs, including samarium NPs (Ghodrat et al., 2019), silver NPs (Venkatadri et al., 2020; Wang et al., 2021a, 2021b), and gold NPS (Alkhatlan et al., 2021), as potential therapeutic agents for the prevention and treatment of different kinds of cancers, have made significant advances in medicine. Bioactive components of ginger including Gingerole (Hu et al., 2020), 6-paradol (Chung et al., 2001), and zingerone (Qian et al., 2021) have been shown to inhibit proliferation of cancer cells in laboratory models. The anti-cancer potential of ginger and its bioactive compounds have been studied in several different types of cancers at the level of cancer cell lines as well as animal models (Shukla et al., 2007; Mahomoodally et al., 2021).

Bismuth (Bi) is one of the most important representative elements of the tin and lead family due to common physical properties (Fal'kovskii, 1968). Bi has been widely used in biological, diagnostic and therapeutic applications (Sun et al., 2004) and Bi oxide (Bi_2O_3) NPs have been proven in many studies (Shahbazi et al., 2020). For example, it has been shown that Bi nanostructures can be used as efficient radiosensitisers on radioresistant cancer cells (Stewart et al., 2016), dual-stimuli responsive platforms for imaging and cancer therapy (Li et al., 2018), and synergistic cancer radiophototherapy (Zhou et al., 2020).

In this article, an attempt has been made to propose a less dangerous, natural and efficient treatment method through the synthesis of Bi_2O_3 NPs using ginger extract based on green chemistry method to selectively inhibit the proliferation of colorectal cancer cells through regulation of phosphatidylinositol-3-kinase (PI3K)/protein kinase B (AKT)/mammalian target of rapamycin (mTOR) (PI3K-AKT-mTOR) signaling pathway as one of the most important molecular pathways controlling cell proliferation and apoptosis. Therefore, in this study, first aqueous extract of ginger was prepared and then Bi_2O_3 NPs were synthesized with the help of ginger extract and green chemistry. In the next step, the physicochemical properties of the synthesized Bi_2O_3 NPs were investigated using various techniques. Finally, the cytotoxicity of Bi_2O_3 NPs against colorectal cancer cell line, HCT116, was studied and compared with ginger extract and bismuth nitrate ($\text{Bi}(\text{NO}_3)_3$) salt. Also, human kidney proximal tubule epithelial cells (HK-2) were used as normal cells as control.

2. Material and methods

2.1. Materials

All chemicals used in this study were analytical grade and dissolved in double distilled (DD) water. Bismuth nitrate ($\text{Bi}(\text{NO}_3)_3$) was obtained from Merck (Shanghai, China). 3-[4,5-dimethylthiazol-2-yl]-2,5-diphenyltetrazolium bromide (MTT), cell culture medium and related materials were purchased from Gibco (Shanghai, China).

2.2. Preparation of ginger root extract

In order to prepare Bi_2O_3 NPs using a green chemistry method, the first ginger extract was prepared. The roots (rhizomes) of the ginger plant were purchased from the market, then thoroughly washed with DD water to remove dirt and contaminants and cut into very small pieces followed by drying at room temperature and making powder. Ginger powder was then dissolved into ethanol and incubated in a shaking incubator at 70°C for 50 min followed by filtration through Whatman® filter papers to obtain pure ginger extract. The

extraction of roots (rhizomes) of the ginger plant yielded 33% (w/v) of the original plant.

2.3. Green synthesis of Bi_2O_3 NPs

For the synthesis of NPs, $\text{Bi}(\text{NO}_3)_3$ salt (2 gr) was mixed with 15 mL DD water and mixed with 30 mL of aqueous extract at 70 °C under constant stirring (200 rpm) for 12 h. By performing redox reactions over a specified period of time, $\text{Bi}(\text{NO}_3)_3$ ions are reduced to Bi_2O_3 NPs, which are observed by gradual changes in the color of the solution. The resulting solution was centrifuged at 6000 rpm for 30 min, washed several times and heated at 450 °C for 6 h to ensure the purity of samples. Finally, the precipitate was dissolved in 5 mL of DD water and physicochemical and morphological studies were performed.

2.4. Phytochemical analysis of the extract

The analysis of bioactive molecules present in the ginger root extract was done for the determination based on the previous report (Das et al., 2020). The total phenolic content in the ginger root extract was determined as gallic acid equivalent by Folin-Ciocalteu polyphenol test (Koşar et al., 2005). The protein content in the ginger root extract was also analyzed by using Lowry's method (Lowry et al., 1951).

2.5. Characterization of Bi_2O_3 NPs

The crystalline nature of the bio-synthesized Bi_2O_3 NPs was studied using the XRD instrument (Rigaku, Tokyo, Japan). The diameter of AuNPs was explored with a Zeiss transmission electron microscope (TEM) at 80 KeV (EM10C, Germany). The UV-Visible spectroscopic study was done to study the surface plasmon resonance of synthesized NPs using Shimadzu apparatus (UV-1800 Japan). The vibrational modes of active components were assessed by FTIR spectroscopy device (Shimadzu, Japan) by preparing the samples in potassium bromide (KBr) under 2:98 ratio of sample: KBr, at a resolution limit of 20 cm^{-1} . Dynamic light scattering (DLS) study was also performed to analyze the size, polydispersity index (PDI), and zeta potential of Bi_2O_3 NPs in solution using a HPPS-5001 Zetasizer (Malvern, UK). All experiments were done at room temperature.

2.6. Cell culture

The HCT116 and HK-2 cells purchased from the Shanghai Institute of Cell Biology (Chinese Academy of Sciences, China), were grown in McCoy's 5a medium and Dulbecco's modified Eagle's medium: nutrient mixture F-12 (DMEM/F12), respectively as described previously (Abalos et al., 2021). For both cells, the media were supplemented with 10% fetal bovine serum (FBS) and 1% antibiotics. Cells were then incubated at 37 °C, 5% CO_2 and 95% humidity and harvested when cells reached 70–80% confluency.

2.7. Cell viability and cytotoxicity assay

Effects of synthesized Bi_2O_3 NPs on HCT116 and HK-2 cells viability were assessed by the MTT assay as described previously (Abalos et al., 2021). Briefly, cells seeded for 24 h were incubated with Bi_2O_3 NPs dispersions prepared in DD water with different concentrations of 1, 5, 10, 100, and 200 $\mu\text{g mL}^{-1}$ for 24 h. Afterwards, the wells were added by 10 μL MTT solution for 4 h at 37 °C, followed by aspiration of culture medium, an addition of 100 μL dimethyl sulfoxide (DMSO). Absorbance of the samples were then read using a spectrophotometer at 570 nm. Based on the MTT assay, the IC_{50} concentrations of Bi_2O_3 NPs on HCT116 and HK-2 cells were determined. Afterwards, the cells were treated with $\text{Bi}(\text{NO}_3)_3$ or ginger extract with similar concentration of Bi_2O_3 NPs for 24 h, and MTT assay was reperformed.

2.8. Lactate dehydrogenase (LDH) assay

Based on the cell viability assay, the IC_{50} concentration of Bi_2O_3 NPs on HCT116 was used in the LDH assay. The membrane damage of HT22 cells incubated with IC_{50} concentration of synthesized Bi_2O_3 NPs was assessed by the LDH assay based on the protocols provided by a commercial kit (Nanjing Jiancheng bioengineering institute, China). Also, the cells were incubated with $\text{Bi}(\text{NO}_3)_3$ and extracts with similar concentration of Bi_2O_3 NPs. Briefly, after treating, the cells were harvested and LDH assay was done based on the concentration of lactate to pyruvate to react with 2,4-dinitrophenylhydrazine for generation of pyruvate dinitrobenzene hydrazine, which is detectable at 450 nm. Absorbance of the samples were then determined using a spectrophotometer.

2.9. Measurement of ROS

1×10^6 cells after being incubated with IC_{50} concentrations of Bi_2O_3 NPs and washed with ice-cold phosphate-buffered saline (PBS) were used for assessing the generation of ROS using 2',7'-dichlorodihydrofluorescein diacetate (DCFH-DA) staining assay as reported previously (Chang et al., 2021). Briefly, HCT116 cells were added by PBS solution supplemented with 30 $\mu\text{mol L}^{-1}$ DCFH-DA and incubated at dark (37 °C for 45 min). Then the cells were washed with PBS and ROS generation was determined by assessing the intensity of dichlorofluorescein (DCF) employing fluorescence microscope (Zeiss, Germany) and flow cytometry (BD, USA).

2.10. Apoptosis assay

Annexin V-fluorescein isothiocyanate (FITC) probe was used for detection of apoptosis in HCT116 cells as described previously (Chang et al., 2021). Briefly, HCT116 cells (1×10^6 cells/well) were plated, cultured, treated with IC_{50} concentrations of Bi_2O_3 NPs for 24 h, collected, washed with PBS, resuspended in binding buffer, and incubated with 5 μL Annexin-V FITC (in the dark for 15 min, room temperature). Finally, the percentage of apoptotic cells relative to the control sample was assessed by flow cytometer (BD, USA).

2.11. Quantitative reverse transcription PCR (RT-qPCR)

RT-qPCR was done to assess the expressions of mRNA based on the previous study (Chang et al., 2021). Briefly, 1 g of the total RNA extracted using TRIzol reagent (TaKaRa, Japan) based on the manufacturer's instruction, was used for synthesis of cDNA.

RT-qPCR was done with a SYBR® Premix Ex Tap™ II Kit using Applied Biosystems Step One Plus Real Time PCR System (Thermo, USA). The protocol used for RT-qPCR was set to previous study (Chang et al., 2021). The primer sequences used for this study are summarized in Table 1. GAPDH was also used as the internal reference and a quantification of mRNA expression was done using a $2^{-\Delta\Delta CT}$ method.

2.12. Statistical analysis

Data obtained triplicate from at least three independent experiments and reported as the mean \pm standard deviation (SD). Comparisons between groups were done by one-way analysis of variance (ANOVA) using SPSS software (Chicago, USA). Differences were reported significant when $p < 0.05$.

3. Results and discussion

3.1. Phytochemical analysis of the ginger root extract

The qualitative analysis of different bioactive compounds in the ginger root extract was done using the methods reported previously (Das et al., 2020). It was found that the protein content in the ginger root extract was about 0.08% of the dry root powder. Also, the total phenolic level in the ginger root extract was 18% of the dry root powder. Based on the determination of total phenolic content of the ginger root extract before (18% of the dry root powder) and after the NP synthesis (12.9 of the dry root powder), it can be proposed that Polyphenol molecules have played a key role in the synthesis of Bi_2O_3 NPs. The total phenolic content of 72 mg gallic acid equivalent from 20 g of dried M. ginger root powder was applied in the fabrication of 150 mg Bi_2O_3 NPs from 2 g $\text{Bi}(\text{NO}_3)_3$ salt solution. The bioactive molecules present in the ginger root extract result in the synthesis and stabilization of the Bi_2O_3 NPs.

An earlier report showed that ginger root extract contains volatile oils, gingerol, diarylheptanoids, protein, polysaccharides, cellulose, soluble sugar, organic acid and inorganic elements (Ansari et al., 2021). Also, it has been shown that ginger root extract contains several flavonoids including quer-

etin, rutin, catechin, epicatechin, kaempferol and naringenin (Ghasemzadeh et al., 2010). Also, it has been also shown that a number of unexplored biomacromolecules are presented in the ginger root extract (Li et al., 2020). Collectively, such data and reports indicate that the ginger root extract could act as a reducing as well as stabilizing agent for the biosynthesis of Bi_2O_3 NPs.

3.2. Characterization of synthesized Bi_2O_3 NPs

The FTIR signal of the synthesized Bi_2O_3 NPs is shown in Fig. 1a. The FTIR technique as a vibration-based spectroscopy can be employed to determine the bioactive compounds involved in the biosynthesis of NPs. The band around 3400 cm^{-1} is indicative of vibration mode of the O-H group, widely presented in bioactive polyphenolic compounds. The band at 420 cm^{-1} is attributed to Bi-O vibration. The fingerprint region between 1000 and 1600 cm^{-1} demonstrates the attachment of the organic molecules to the synthesized Bi_2O_3 NPs. This data reflects the involvement of the bioactive compounds in the biosynthesis of Bi_2O_3 NPs. The finding of FTIR study was in good agreement with previous studies (Mallahi et al., 2014; Das et al., 2020; Motakef-Kazemi and Yaqoubi, 2020).

The UV-Vis absorption spectrum of the ginger root extract and synthesized Bi_2O_3 NPs is depicted in Fig. 1b. It was shown that the ginger root extract shows a λ_{max} around 400 nm, revealing the presence of phytochemicals, whereas the synthesized Bi_2O_3 NPs depicts a λ_{max} of around 268 nm, which is in good agreement with previous study (Motakef-Kazemi and Yaqoubi, 2020; Das et al., 2020). Also, in the absorption spectrum of the Bi_2O_3 NPs, the adsorption spectrum of phytochemicals is remarkably reduced and red shifted, due to alterations in poly-hydroxyl agents involved in the reduction and stability of the Bi_2O_3 NPs.

X-ray diffraction measurement (XRD) was also used to explore the crystalline structure of Bi_2O_3 NPs in the 2θ range 20 – 60° after the green synthesis route (Fig. 1c). Eight clear peaks were observed in the XRD pattern of synthesized Bi_2O_3 NPs at 2θ values of 25.81° , 26.61° , 27.72° , 28.89° , 31.98° , 34.06° , 38.01° , and 46.05° corresponding to 002, 111, 120, 012, 122, 200, 112, and 041 crystalline phases indexed as monoclinic α - Bi_2O_3 NPs (JCPDS card No. 41-1449). This data is also similar to the previously reported XRD outcomes for Bi_2O_3 NPs (Raza et al., 2015; Motakef-Kazemi and Yaqoubi, 2020).

Transmission electron microscopy (TEM) analysis was also done to visualize the size and morphology of synthesized Bi_2O_3 NPs (Fig. 1d). The TEM image showed that the synthesized

Table 1 Primers used for RT-qPCR analysis.

Gene	Forward (5–3')	Reverse (5–3')
PI3K	CTCTACGGAGTGTCCATATACCTG	CATTAAATGCTTCGATAGCCGTTCT
AKT	GTGTGGCAGGATGTGTATGAGAACA	CTGAGTAGGAGAACTGGGGGAAGT
mTOR	GGACTTTGGGAGAAACGAAGATGG	CGGGTGAGGTAACAGGATAGTGGA
Bax	CCAGGATCGAGCAGGGAGGA	GTCCGTGTCCACGTACAGCAA
Bcl-2	GCTACCGTCCTGACTCCGCA	ATCCTTTCCAGTTCACCCC
Caspase-3	CGGAGCTCGACTGTGGCATT	GGATGCGCATGACCCCGTCC
GAPDH	AGAAGGTTGTATGGCGAGCATC	CGAAGGTGGAAGAGTGGGAGTTG

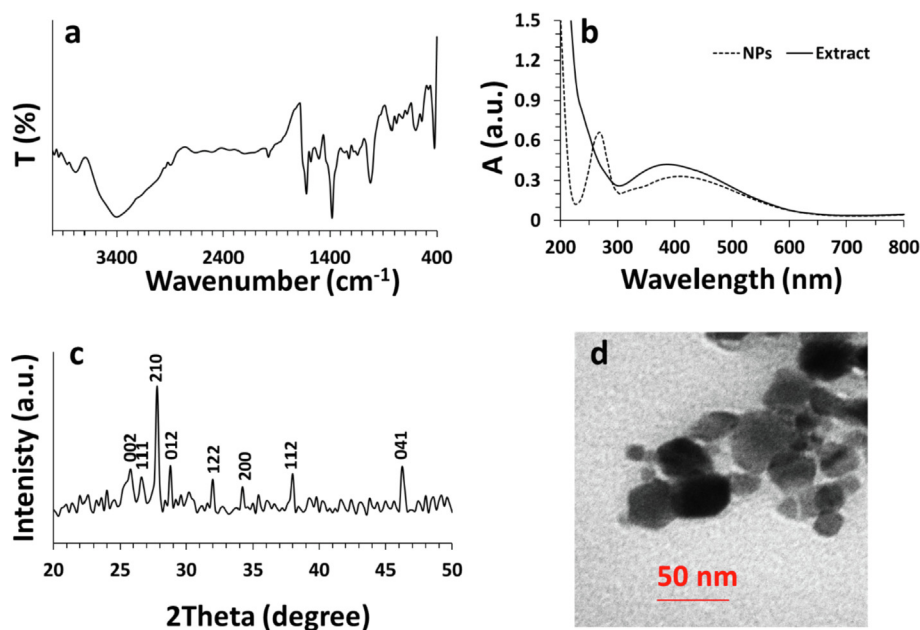


Fig. 1 Characterization of synthesized Bi_2O_3 NPs from Ginger (*Zingiber officinale*) root (rhizome) extract. (a) Fourier transform-infrared spectroscopy (FTIR), (b) UV-visible, (c) X-ray diffraction (XRD), (d) transmission electron microscopy (TEM) analyses.

Bi_2O_3 NPs have a size range of 20–50 nm with a mean size of around 35 nm and an almost spherical morphology. The relative agglomeration of synthesized NPs is usually stimulated by evaporation of solution during the sample preparation.

The dynamic light scattering (DLS) analysis was also performed to find out the size and zeta potential of synthesized Bi_2O_3 NPs in DD water. It was found that synthesized Bi_2O_3 NPs have a size of about 71.19 nm (PDI of 0.179) and a zeta potential value of -44.39 mV. The narrow size distribution and high zeta potential value at ambient temperature not only confirmed the other characterization outcomes, but also revealed the good colloidal stability of synthesized Bi_2O_3 NPs.

3.3. Cellular assays

3.3.1. Viability and membrane leakage assays

The present study was then aimed to evaluate the anticancer and cytotoxicity of synthesized Bi_2O_3 NPs. It was revealed that the synthesized NPs using plant extracts can be used as a source of potential anticancer agents as shown by the MTT assay (Fig. 2a). Synthesized Bi_2O_3 NPs using ginger extract in the present paper displayed strong anticancer effect against HCT116 with IC_{50} value of $48.93 \pm 4.27 \mu\text{g mL}^{-1}$ but low cytotoxicity against normal HK-2 cells with IC_{50} value of $>200 \mu\text{g mL}^{-1}$. Therefore, for further experiments, the cells were treated with $50 \mu\text{g mL}^{-1}$ Bi_2O_3 NPs or other compounds including extract or Bi salt. This preliminary study indicated the selective anticancer effects of synthesized Bi_2O_3 NPs using ginger extract, enhancing their potential for advancement as anticancer platforms. Therefore, this is the first report to study the potent anticancer activity of synthesized Bi_2O_3 NPs against cancer cell line. Previous investigations have shown the biogenic Bi NPs with a particle size between 20 and 120 nm show potential anticancer effect against cancer cell lines (A549 and

MCF-7) and low cytotoxicity against normal fibroblast cells (3 T3) with IC_{50} values of around $11 \mu\text{g mL}^{-1}$, $36 \mu\text{g mL}^{-1}$, and $43 \mu\text{g mL}^{-1}$, respectively (Shakibaie et al., 2018). Also, it has been found that samarium NPs fabricated by ginger extract with a size of around 60 nm show potential anticancer effects against HCT116 colorectal cancer cells with an IC_{50} value of around $32 \mu\text{g mL}^{-1}$ (Ghodrat et al., 2019).

Also, it was shown that, although ginger extract with a concentration of $50 \mu\text{g mL}^{-1}$ did not induce a significant cytotoxic effect in both HCT116 colorectal cancer and normal HK-2 cells (Fig. 2b), $\text{Bi}(\text{NO}_3)_3$ salt with the similar concentration to extract and Bi_2O_3 NPs, $50 \mu\text{g mL}^{-1}$, triggered significant ($***P < 0.001$) anticancer and cytotoxic effects against both cancerous and non-cancerous cells. His data indicated that one of the possible reasons for the cytotoxic effects of NPs is the release of ions for the surface of the NPs over time (Wang et al., 2016). Therefore, it can be claimed that, although Bi salt could induce anticancer effects in a non-selective manner, Bi_2O_3 NPs induced a selective anticancer effect against HCT116 colorectal cancer cells, which is probably due to higher cellular uptake of NPs in cancer cells relative to normal cells (Sharifi et al., 2019).

LDH assay, a marker of membrane leakage, also verified the MTT assay. In fact, it was shown that the most membrane leakage ($***P < 0.001$) is induced by $\text{Bi}(\text{NO}_3)_3$ salt in both HCT116 colorectal cancer and normal HK-2 cells (Fig. 2c), whereas the LDH release induced by synthesized Bi_2O_3 NPs using ginger extract was done based on a selective manner against cancer cells ($**P < 0.01$). Also, it was seen after treatment of cells with $50 \mu\text{g mL}^{-1}$ ginger extract, no remarkable LDH release was detected.

Previous reported that bioactive compounds (Mao et al., 2019) found in ginger inhibit the proliferation of different tumor cells (Mahomoodally et al., 2021), including colorectal cancer cells (Abdullah et al., 2010; Su et al., 2019). Also, it

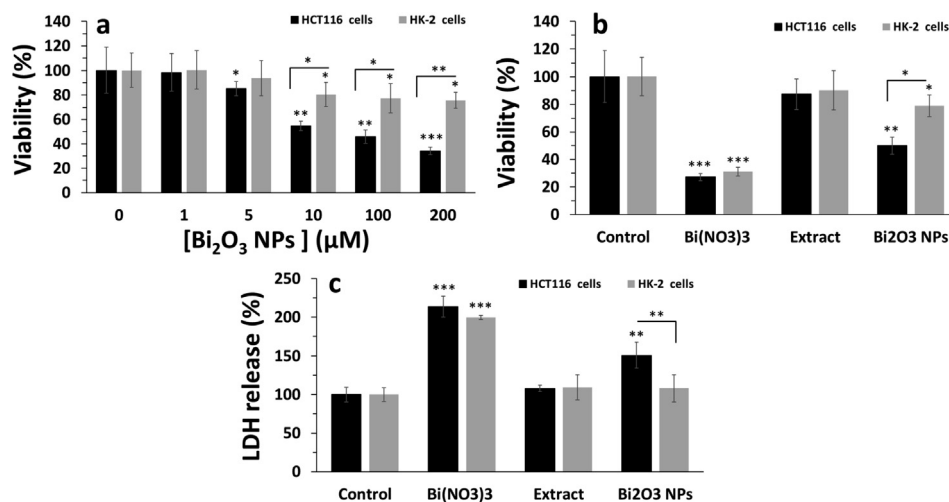


Fig. 2 Cellular assays after exposure of HCT116 colorectal cancer and normal HK-2 cells to synthesized Bi₂O₃ NPs using Ginger (*Zingiber officinale*) root (rhizome) extract for 24 h. (a) MTT assay for determination of cell viability upon exposure to different concentrations of synthesized Bi₂O₃ NPs, (b) MTT assay for determination of cell viability upon exposure of cells to a single concentration (equal to IC₅₀ concentration of Bi₂O₃ NPs against HCT116 colorectal cancer, about 50 µg mL⁻¹) of ginger extract or Bi(NO₃)₃ or Bi₂O₃ NPs, (c) LDH assay for determination of membrane leakage upon exposure of cells to a single concentration (equal to IC₅₀ concentration of Bi₂O₃ NPs against HCT116 colorectal cancer, about 50 µg mL⁻¹) of ginger extract or Bi(NO₃)₃ or Bi₂O₃ NPs. *P < 0.05, **P < 0.01, P < 0.001, relative to control samples, #P < 0.05, ##P < 0.01, relative to determined control cells.

has been reported that Bi NPs can be used both alone and in conjugation with anticancer drugs for development of anticancer platforms (Faghfoori et al., 2020; Cabral-Romero et al., 2020). These reports support the data from the present study for anticancer activity of Bi₂O₃ NPs synthesized using rhizome extracts of ginger. Other than ginger, *Moringa oleifera* leaves extract (Das et al., 2020) and *Mentha pulegium* extract (Motakef-Kazemi and Yaqoubi, 2020) also used for Bi₂O₃ NPs synthesis with different biological implementations. In a study by Motakef-Kazemi and Yaqoubi (2020), who fabricated Bi₂O₃ NPs from *Mentha pulegium* extract and reported its anticancer activity (Motakef-Kazemi and Yaqoubi, 2020). Also, it has been reported that gold (Alkhatlan et al., 2021) and silver NPs (Wang et al., 2021a, 2021b) synthesized by ginger extract can be used as potential anticancer agents. For example, it was reported that the silver NPs synthesized by using ginger extract had an average size of round 19 nm and anti-pancreatic cancer characteristics with IC₅₀ values of around 300, 310, and 220 µg mL⁻¹ against AsPC-1, PANC-1, and MIA PaCa-2 cancer cells, respectively (Wang et al., 2021a, 2021b).

3.3.2. ROS and apoptosis assays

The IC₅₀ concentration of Bi₂O₃ NPs was added to the HCT116 colorectal cancer cells for 24 h and generation of intracellular ROS was explored by flow cytometry. The flow cytometry analysis indicated that the mean fluorescence intensity of dichlorofluorescein (DCF) was around 83.66 ± 5.03 a. u. untreated control cells (Fig. 3a), which was significantly (**P < 0.001) increased to 791.33 ± 37.07 a.u. after incubation of cells with Bi₂O₃ NPs for 24 h. This data shows the generation of ROS in Bi₂O₃ NPs-treated HCT116 colorectal cancer cells.

Furthermore, it was found that the percentage of Annexin-V FITC⁺ cells in untreated control cells (Fig. 3b) was around 3.49 ± 0.57, which was significantly (**P < 0.001) increased

to 63.31 ± 4.67 after incubation of cells with Bi₂O₃ NPs for 24 h, indicating the induction of apoptosis in Bi₂O₃ NPs-treated HCT116 colorectal cancer cells.

In general, it can be claimed that synthesized Bi₂O₃ NPs using ginger extract can selectively inhibit the proliferation of cancer cells through potential penetration in HCT116 colorectal cancer cells, generation of ROS, and induction of apoptosis.

Indeed, it has been found that oxidative stress regulation and ROS-triggered cytotoxicity in cancer cells mediated by plant-derived agents (Vallejo et al., 2017). Also, it has been shown that synthesized silver NPs using plant extract induced apoptotic effect in colon cancer mediated by ROS (Satapathy et al., 2015). Furthermore, it has been indicated that synthesized gold NPs triggered anticancer effects in human colorectal cancer cells through apoptosis-mediated by oxidative stress (Vairavel et al., 2020). In fact, it can be deduced that plant extract (compound)-assisted NPs stimulate apoptosis via oxidative stress in human cancer cell lines (Hamida et al., 2020; Raj et al., 2020).

3.3.3. Effects of apoptosis induced by synthesized Bi₂O₃ NPs on HCT116 cells evidenced by RT-qPCR analysis

To further explore synthesized Bi₂O₃ NPs-triggered apoptosis in HCT116 colorectal cancer cells, the mRNA expressions of Bax, Bcl-2 and Caspase-3, well-known markers of apoptosis, were determined by the RT-qPCR (Fig. 4) analysis. After 50 µg mL⁻¹ Bi₂O₃ NPs exposure to HCT116 colorectal cancer cells for 24 h, the mRNA expression (Fig. 4) of Bax and Caspase-3, apoptotic markers, was increased, and Bcl-2 mRNA expression, an antiapoptotic marker, was reduced. Also, it was seen that the expression ratio of Bax/Bcl-2 at mRNA level was increased after treatment of cells with 50 µg mL⁻¹ Bi₂O₃ NPs, indicating the induction of apoptosis. These data further revealed the induction of apoptosis in

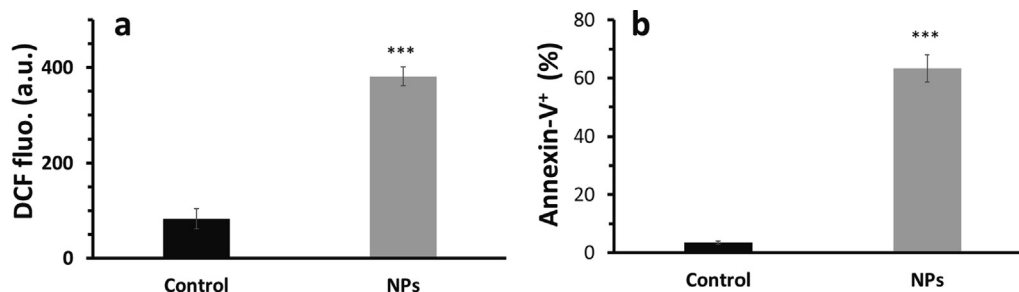


Fig. 3 ROS and apoptosis assays in HCT116 colorectal cancer after exposure to synthesized Bi_2O_3 NPs (IC_{50} concentration, $50 \mu\text{g mL}^{-1}$) using Ginger (*Zingiber officinale*) root (rhizome) extract for 24 h determined by flow cytometry. (a) ROS assay for determination of ROS in Bi_2O_3 NPs -treated HCT116 colorectal cancer cells as determined by DCFH2/DCF probe, (b) apoptosis assay in Bi_2O_3 NPs -treated HCT116 colorectal cancer cells as determined by Annexin-V FITC probe. *** $P < 0.001$, relative to control samples.

HCT116 colorectal cancer cells triggered by Bi_2O_3 NPs ($50 \mu\text{g mL}^{-1}$).

It has been also shown that biogenic metal NPs can induce anticancer effects through the stimulation of oxidative stress, mitochondrial dysfunction and apoptosis (Maity et al., 2018). Also, it has been reported that synthesized gold NPs using leaf *Panax notoginseng* induce intrinsic apoptotic gene expressions in pancreatic cancer cell lines mediated by ROS. Therefore, it can be claimed that plant extract-synthesized NPs induces mitochondrial apoptosis through regulation of Bax, Bcl-2, caspase mRNA via oxidative stress in cancer cell lines (Raj et al., 2020).

3.3.4. Investigation of PI3K/AKT/mTOR signaling pathway at mRNA level

To investigate the potential mechanism by which Bi_2O_3 NPs induces apoptosis in HCT116 colorectal cancer cells, the mRNA expression of the PI3K/AKT/mTOR signaling pathway was analyzed using the RT-qPCR assay. Compared with the control samples, the reduced mRNA expression of PI3K, AKT and mTOR was detected in the Bi_2O_3 NPs ($50 \mu\text{g mL}^{-1}$)-treated group (Fig. 5). In fact, the changes in the mRNA indicated that Bi_2O_3 NPs may induce their anticancer effects through regulation of PI3K/AKT/mTOR signaling pathway.

Treatment for patients with metastatic or recurrent colorectal cancer usually includes radiation therapy, chemotherapy,

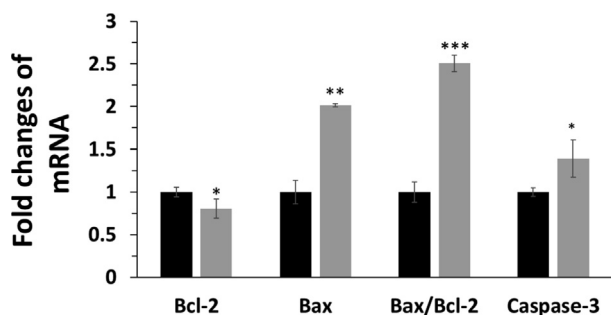


Fig. 4 Apoptosis assay in HCT116 colorectal cancer cells after exposure to synthesized Bi_2O_3 NPs (IC_{50} concentration, $50 \mu\text{g mL}^{-1}$) using Ginger (*Zingiber officinale*) root (rhizome) extract for 24 h determined by RT-qPCR analysis by exploring the mRNA expression level of Bax, Bcl2, and Caspase-3. * $P < 0.05$, ** $P < 0.01$, *** $P < 0.001$, relative to control samples. Black: control cells, Gery: NP-treated HCT116 colorectal cancer cells.

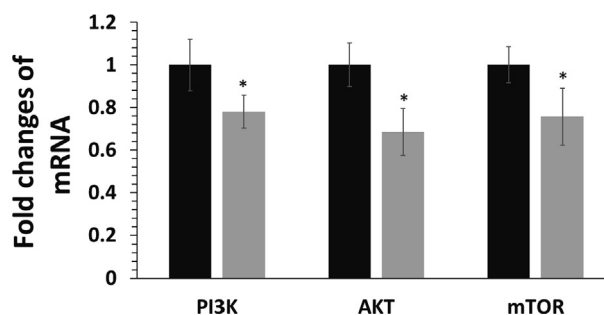


Fig. 5 Exploring the regulation of the PI3K/AKT/mTOR signaling pathway in HCT116 colorectal cancer cells after exposure to synthesized Bi_2O_3 NPs (IC_{50} concentration, $50 \mu\text{g mL}^{-1}$) using Ginger (*Zingiber officinale*) root (rhizome) extract for 24 h determined by RT-qPCR assay. * $P < 0.05$ relative to control samples. Black: control cells, Gery: NP-treated HCT116 colorectal cancer cells.

endocrine therapy, or a combination of these approaches, in an effort to inhibit the growth of the cancer (Ayanian et al., 2003). The cancer response to these treatments varies, but is often moderate. Therefore, new promising treatments are needed to improve therapeutic outcomes. The PI3K/AKT/mTOR signaling pathway within a colorectal cancer cell is involved in the growth of cancer cells (Johnson et al., 2010), and various drugs/NPs (Pandurangan et al., 2013; Bahrami et al., 2018; Narayanankutty, 2019) have been developed to target this pathway to reduce the growth of colorectal cancer cells.

The PI3K, AKT, and mTOR inhibitors can play a key role in the inhibition of proliferation of cancer cells (Narayanankutty, 2019). Several NPs-based anticancer agents including zinc oxide NPs (Roy et al., 2014), nickel NPs (Wu et al., 2020), and copper oxide NPs (Chen et al., 2021) have been reported to inhibit PI3K/AKT/mTOR signaling pathway. These inhibitors can be given alone or in combination with other cancer medications including chemotherapy or endocrine therapy.

4. Conclusion

In this study, ginger root extract was used for green synthesis of Bi_2O_3 NPs. Different characterization techniques were used for analysis of synthesized Bi_2O_3 NPs, whereas FTIR, UV-Visible, and XRD tech-

niques indicated the presence of Bi-O vibration, a λ_{\max} of around 268 nm, and crystalline phases in the structure of synthesized Bi₂O₃ NPs. Also, TEM and DLS assays showed that Bi₂O₃ NPs have a spherical with a mean size of 35 nm, a hydrodynamic radius of about 71.19 nm (PDI of 0.179), and a zeta potential value of -44.39 mV. It was also found that synthesized Bi₂O₃ NPs induce selective anticancer effects against HCT116 colorectal cancer cells via apoptosis mediated by regulation of PI3K / AKT / mTOR signaling pathway. Overall, the results obtained in this study indicate that the synthesized Bi₂O₃ NPs using ginger extract have shown favorable selective anticancer effects and probably can be used as a suitable drug in the treatment of colorectal cancer cells. However, further studies, including *in vivo* studies and clinical trials, are needed to understand the mechanism of action of this drug and its health for cancer patients.

Declaration of Competing Interest

The authors declare that they have no known competing financial interests or personal relationships that could have appeared to influence the work reported in this paper.

Acknowledgment

We do appreciate Dr. Majid Sharfi for helpful assistance in the editing, experimental design and discussion of the paper.

References

- Abalos, N.N., Ebajo Jr, V.D., Camacho, D.H., Jacinto, S.D., 2021. Cytotoxic and Apoptotic Activity of Aglaforbesin Derivative Isolated from *Aglaia loheri* Merr. on HCT116 Human Colorectal Cancer Cells. *Asian Pacific J. Cancer Prevent.: APJCP* 22 (1), 53.
- Abdullah, S., Abidin, S.A., Murad, N.A., Makpol, S., Ngah, W.Z., Yusof, Y.A., 2010. Ginger extract (*Zingiber officinale*) triggers apoptosis and G0/G1 cells arrest in HCT 116 and HT 29 colon cancer cell lines. *Afr. J. Biochem. Res.* 4 (5), 134–142.
- Alkhatlan, A.H., Al-Abdulkarim, H.A., Khan, M., Khan, M., Alkholief, M., Alshamsan, A., Almomen, A., Albekairi, N., Alkhatlan, H.Z., Siddiqui, M.R., 2021. Evaluation of the Anticancer Activity of Phytomolecules Conjugated Gold Nanoparticles Synthesized by Aqueous Extracts of *Zingiber officinale* (Ginger) and *Nigella sativa* L. Seeds (Black Cumin). *Materials* 14 (12), 3368.
- Ansari, F.R., Chodhary, K.A., Ahad, M., 2021. A review on ginger (*Zingiber officinale* Rosc) with unani perspective and modern pharmacology. *J. Med. Plants* 9 (3), 101–104.
- Ayanian, J.Z., Zaslavsky, A.M., Fuchs, C.S., Guadagnoli, E., Creech, C.M., Cress, R.D., O'Connor, L.C., West, D.W., Allen, M.E., Wolf, R.E., Wright, W.E., 2003. Use of adjuvant chemotherapy and radiation therapy for colorectal cancer in a population-based cohort. *J. Clin. Oncol.* 21 (7), 1293–1300.
- Bahrami, A., Khzaei, M., Hasanzadeh, M., ShahidSales, S., Joudi Mashhad, M., Farazestanian, M., Sadeghnia, H.R., Rezayi, M., Maftouh, M., Hassanian, S.M., Avan, A., 2018. Therapeutic potential of targeting PI3K/AKT pathway in treatment of colorectal cancer: rational and progress. *J. Cell. Biochem.* 119 (3), 2460–2469.
- Cabral-Romero, C., Solis-Soto, J.M., Sánchez-Pérez, Y., Pineda-Aguilar, N., Meester, I., Pérez-Carrillo, E., Nakagoshi-Cepeda, S. E., Sánchez-Nájera, R.I., Nakagoshi-Cepeda, M.A., Hernandez-Delgado, R., Chellam, S., 2020. Antitumor activity of a hydrogel loaded with lipophilic bismuth nanoparticles on cervical, prostate, and colon human cancer cells. *Anticancer Drugs* 31 (3), 251–259.
- Chang, X., Wang, X., Li, J., Shang, M., Niu, S., Zhang, W., Li, Y., Sun, Z., Gan, J., Li, W., Tang, M., 2021. Silver nanoparticles induced cytotoxicity in HT22 cells through autophagy and apoptosis via PI3K/AKT/mTOR signaling pathway. *Ecotoxicol. Environ. Saf.* 15, (208) 111696.
- Chen, H., Feng, X., Gao, L., Mickymaray, S., Paramasivam, A., Abdulaziz Alfaiz, F., Almasmoum, H.A., Ghaith, M.M., Almai-mani, R.A., Aziz Ibrahim, I.A., 2021. Inhibiting the PI3K/AKT/mTOR signalling pathway with copper oxide nanoparticles from *Houttuynia cordata* plant: attenuating the proliferation of cervical cancer cells. *Artif. Cells Nanomed. Biotechnol.* 49 (1), 240–249.
- Chung, W.Y., Jung, Y.J., Surh, Y.J., Lee, S.S., Park, K.K., 2001. Antioxidative and antitumor promoting effects of [6]-paradol and its homologs. *Mutation Research/Genetic Toxicol. Environ. Mutagenesis* 496 (1–2), 199–206.
- Coelho, M.C., Torrão, G., Emami, N., 2012. Nanotechnology in automotive industry: research strategy and trends for the future—small objects, big impacts. *J. Nanosci. Nanotechnol.* 12 (8), 6621–6630.
- Das, P.E., Majdalawieh, A.F., Abu-Yousef, I.A., Narasimhan, S., Poltronieri, P., 2020. Use of a hydroalcoholic extract of *moringa oleifera* leaves for the green synthesis of bismuth nanoparticles and evaluation of their anti-microbial and antioxidant activities. *Materials* 13 (4), 876.
- Ghasemzadeh, A., Jaafar, H.Z., Rahmat, A., 2010. Identification and concentration of some flavonoid components in Malaysian young ginger (*Zingiber officinale* Roscoe) varieties by a high performance liquid chromatography method. *Molecules* 15 (9), 6231–6243.
- Ghodrat, I.Z., Divsalar, A., Ayrian, S., Saeidifar, M., 2019. Evaluation of the anticancer effects of Samarium nanoparticles synthesized by extract of ginger on HCT116 colorectal cancer cells. *J. Cell Tissue* 10 (4), 202–213.
- Faghfoori, M.H., Nosrati, H., Rezaeejam, H., Charmi, J., Kaboli, S., Johari, B., Danafar, H., 2020. Anticancer effect of X-Ray triggered methotrexate conjugated albumin coated bismuth sulfide nanoparticles on SW480 colon cancer cell line. *Int. J. Pharm.* 30, (582) 119320.
- Fal'kovskii, L.A., 1968. Physical properties of bismuth. *Soviet Physics Uspekhi.* 11 (1), 1.
- Gingras, D., Bêliveau, R., 2011. Colorectal cancer prevention through dietary and lifestyle modifications. *Cancer Microenviron.* 4 (2), 133–139.
- Haggar, F.A., Boushey, R.P., 2009. Colorectal cancer epidemiology: incidence, mortality, survival, and risk factors. *Clinics Colon Rectal Surg.* 22 (04), 191–197.
- Hamida, R.S., Albasher, G., Bin-Meferij, M.M., 2020. Oxidative stress and apoptotic responses elicited by nostoc-synthesized silver nanoparticles against different cancer cell lines. *Cancers* 12 (8), 2099.
- Hu, S.M., Yao, X.H., Hao, Y.H., Pan, A.H., Zhou, X.W., 2020. 8-Gingerol regulates colorectal cancer cell proliferation and migration through the EGFR/STAT/ERK pathway. *Int. J. Oncol.* 56 (1), 390–397.
- Iravani, S., Korbekandi, H., Mirmohammadi, S.V., Zolfaghari, B., 2014. Synthesis of silver nanoparticles: chemical, physical and biological methods. *Res. Pharm. Sci.* 9 (6), 385.
- Jadoun, S., Arif, R., Jangid, N.K., Meena, R.K., 2021. Green synthesis of nanoparticles using plant extracts: A review. *Environ. Chem. Lett.* 19 (1), 355–374.
- Jamkhande, P.G., Ghule, N.W., Bamer, A.H., Kalaskar, M.G., 2019. Metal nanoparticles synthesis: An overview on methods of preparation, advantages and disadvantages, and applications. *J. Drug Delivery Sci. Technol.* 1, (53) 101174.
- Johnson, S.M., Gulhati, P., Rampy, B.A., Han, Y., Rychahou, P.G., Doan, H.Q., Weiss, H.L., Evers, B.M., 2010. Novel expression patterns of PI3K/Akt/mTOR signaling pathway components in colorectal cancer. *J. Am. Coll. Surg.* 210 (5), 767–776.
- Koşar, M., Dorman, H.J., Hiltunen, R., 2005. Effect of an acid treatment on the phytochemical and antioxidant characteristics of extracts from selected Lamiaceae species. *Food Chem.* 91 (3), 525–533.

- Li, X., Chen, W., Chang, Q., Zhang, Y., Zheng, B., Zeng, H., 2020. Structural and physicochemical properties of ginger (*Rhizoma curcumae longae*) starch and resistant starch: A comparative study. *Int. J. Biol. Macromol.* 1 (144), 67–75.
- Li, Z., Hu, Y., Miao, Z., Xu, H., Li, C., Zhao, Y., Li, Z., Chang, M., Ma, Z., Sun, Y., Besenbacher, F., 2018. Dual-stimuli responsive bismuth nanoraspberries for multimodal imaging and combined cancer therapy. *Nano Lett.* 18 (11), 6778–6788.
- Lowry, O.H., Roserough, N.J., Farr, A.L., Randall, R.J., 1951. Protein measurement with the folin phenol reagent. *J. Biol. Chem.* 193, 265–275.
- Mahomoodally, M.F., Aumeeruddy, M.Z., Rengasamy, K.R., Roshan, S., Hammad, S., Pandohee, J., Hu, X., Zengin, G., 2021. Ginger and its active compounds in cancer therapy: From folk uses to nano-therapeutic applications. In: *Seminars in Cancer Biology*. Academic Press, pp. 140–149.
- Mallahi, M., Shokuhfar, A., Vaezi, M.R., Esmailirad, A., Mazinani, V., 2014. Synthesis and characterization of bismuth oxide nanoparticles via sol-gel method. *AJER* 3, 162–165.
- Mao, Q.Q., Xu, X.Y., Cao, S.Y., Gan, R.Y., Corke, H., Li, H.B., 2019. Bioactive compounds and bioactivities of ginger (*Zingiber officinale* Roscoe). *Foods* 8 (6), 185.
- Maity, P., Bepari, M., Pradhan, A., Baral, R., Roy, S., Choudhury, S. M., 2018. Synthesis and characterization of biogenic metal nanoparticles and its cytotoxicity and anti-neoplasticity through the induction of oxidative stress, mitochondrial dysfunction and apoptosis. *Colloids Surf., B* 1 (161), 111–120.
- Mittal, A.K., Chisti, Y., Banerjee, U.C., 2013. Synthesis of metallic nanoparticles using plant extracts. *Biotechnol. Adv.* 31 (2), 346–356.
- Mitchell, M.J., Billingsley, M.M., Haley, R.M., Wechsler, M.E., Peppas, N.A., Langer, R., 2021. Engineering precision nanoparticles for drug delivery. *Nat. Rev. Drug Discovery* 20 (2), 101–124.
- Motakef-Kazemi, N., Yaqoubi, M., 2020. Green synthesis and characterization of bismuth oxide nanoparticle using mentha pulegium extract. *Iranian J. Pharm. Res.: IJPR* 19 (2), 70.
- Mullins, C.S., Eisold, S., Klar, E., Linnebacher, M., 2011. Multidrug-resistance proteins are weak tumor associated antigens for colorectal carcinoma. *BMC Immunol.* 12 (1), 1–9.
- Narayanankutty, A., 2019. PI3K/Akt/mTOR pathway as a therapeutic target for colorectal cancer: a review of preclinical and clinical evidence. *Curr. Drug Targets* 20 (12), 1217–1226.
- Pandurangan, A.K., 2013. Potential targets for prevention of colorectal cancer: a focus on PI3K/Akt/mTOR and Wnt pathways. *Asian Pac. J. Cancer Prev.* 14 (4), 2201–2205.
- Powers, K.W., Palazuelos, M., Moudgil, B.M., Roberts, S.M., 2007. Characterization of the size, shape, and state of dispersion of nanoparticles for toxicological studies. *Nanotoxicology* 1 (1), 42–51.
- Qian, S., Fang, H., Zheng, L., Liu, M., 2021. Zingerone suppresses cell proliferation via inducing cellular apoptosis and inhibition of the PI3K/AKT/mTOR signaling pathway in human prostate cancer PC-3 cells. *J. Biochem. Mol. Toxicol.* 35, (1) e22611.
- Raj, R.K., 2020. β -Sitosterol-assisted silver nanoparticles activates Nrf2 and triggers mitochondrial apoptosis via oxidative stress in human hepatocellular cancer cell line. *J. Biomed. Mater. Res. Part A* 108 (9), 1899–1908.
- Raza, W., Haque, M.M., Muneer, M., Harada, T., Matsumura, M., 2015. Synthesis, characterization and photocatalytic performance of visible light induced bismuth oxide nanoparticle. *J. Alloys. Compd.* 648, 641–660.
- Roy, R., Singh, S.K., Chauhan, L.K., Das, M., Tripathi, A., Dwivedi, P.D., 2014. Zinc oxide nanoparticles induce apoptosis by enhancement of autophagy via PI3K/Akt/mTOR inhibition. *Toxicol. Lett.* 227 (1), 29–40.
- Sanna, V., Sechi, M., 2020. Therapeutic potential of targeted nanoparticles and perspective on nanotherapies. *ACS Med. Chem. Lett.* 11 (6), 1069–1073.
- Satapathy, S.R., Mohapatra, P., Das, D., Siddharth, S., Kundu, C.N., 2015. The apoptotic effect of plant based nanosilver in colon cancer cells is a p53 dependent process involving ROS and JNK cascade. *Pathol. Oncol. Res.* 21 (2), 405–411.
- Soni, M., Mehta, P., Soni, A., Goswami, G.K., 2018. Green nanoparticles: Synthesis and applications. *IOSR J. Biotechnol. Biochem.* 4, 78–83.
- Shahbazi, M.A., Faghfour, L., Ferreira, M.P., Figueiredo, P., Maleki, H., Sefat, F., Hirvonen, J., Santos, H.A., 2020. The versatile biomedical applications of bismuth-based nanoparticles and composites: therapeutic, diagnostic, biosensing, and regenerative properties. *Chem. Soc. Rev.* 49 (4), 1253–1321.
- Shakibaie, M., Amiri-Moghadam, P., Ghazanfari, M., Adeli-Sardou, M., Jafari, M., Foroofanfar, H., 2018. Cytotoxic and antioxidant activity of the biogenic bismuth nanoparticles produced by *Delftia* sp. *SFG. Mater. Res. Bull.* 1 (104), 155–163.
- Sharifi, M., Attar, F., Saboury, A.A., Akhtari, K., Hooshmand, N., Hasan, A., El-Sayed, M.A., Falahati, M., 2019. Plasmonic gold nanoparticles: Optical manipulation, imaging, drug delivery and therapy. *J. Control. Release* 1 (311), 170–189.
- Shukla, Y., Singh, M., 2007. Cancer preventive properties of ginger: a brief review. *Food Chem. Toxicol.* 45 (5), 683–690.
- Su, P., Veeraraghavan, V.P., Krishna Mohan, S., Lu, W., 2019. A ginger derivative, zingerone—a phenolic compound—induces ROS-mediated apoptosis in colon cancer cells (HCT-116). *J. Biochem. Mol. Toxicol.* 33, (12) e22403.
- Sun, H., Zhang, L., Szeto, K.Y., 2004. Bismuth in medicine. *Met. Ions Biol. Syst.* 1 (41), 333–378.
- Stewart, C., Konstantinov, K., McKinnon, S., Guatelli, S., Lerch, M., Rosenfeld, A., Tehei, M., Corde, S., 2016. First proof of bismuth oxide nanoparticles as efficient radiosensitisers on highly radioresistant cancer cells. *Phys. Med.* 32 (11), 1444–1452.
- Vallejo, M.J., Salazar, L., Grijalva, M., 2017. Oxidative stress modulation and ROS-mediated toxicity in cancer: a review on in vitro models for plant-derived compounds. *Oxid. Med. Cell. Longevity* 24, 2017.
- Venkatadri, B., Shanparvish, E., Rameshkumar, M.R., Arasu, M.V., Al-Dhabi, N.A., Ponnusamy, V.K., Agastian, P., 2020. Green synthesis of silver nanoparticles using aqueous rhizome extract of *Zingiber officinale* and *Curcuma longa*: In-vitro anti-cancer potential on human colon carcinoma HT-29 cells. *Saudi J. Biol. Sci.* 27 (11), 2980–2986.
- Vairavel, M., Devaraj, E., Shanmugam, R., 2020. An eco-friendly synthesis of *Enterococcus* sp.-mediated gold nanoparticle induces cytotoxicity in human colorectal cancer cells. *Environ. Sci. Pollut. Res.* 27 (8), 8166–8175.
- Wang, D., Lin, Z., Wang, T., Yao, Z., Qin, M., Zheng, S., Lu, W., 2016. Where does the toxicity of metal oxide nanoparticles come from: the nanoparticles, the ions, or a combination of both? *J. Hazard. Mater.* 5 (308), 328–334.
- Wang, H., Huang, Y., 2020. Combination therapy based on nano codelivery for overcoming cancer drug resistance. *Med. Drug Discovery* 1, (6) 100024.
- Wu, Y., Ma, J., Sun, Y., Tang, M., Kong, L., 2020. Effect and mechanism of PI3K/AKT/mTOR signaling pathway in the apoptosis of GC-1 cells induced by nickel nanoparticles. *Chemosphere* 1, (255) 126913.
- Wang, J.Q., Yang, Y., Cai, C.Y., Teng, Q.X., Cui, Q., Lin, J., Assaraf, Y.G., Chen, Z.S., 2021. Multidrug resistance proteins (MRPs): Structure, function and the overcoming of cancer multidrug resistance. *Drug Resist. Updates* 1, (54) 100743.

- Wang, Y., Chinnathambi, A., Nasif, O., Alharbi, S.A., 2021. Green synthesis and chemical characterization of a novel anti-human pancreatic cancer supplement by silver nanoparticles containing *Zingiber officinale* leaf aqueous extract. *Arabian J. Chem.* 14, (4) 103081.
- Zhou, R., Liu, X., Wu, Y., Xiang, H., Cao, J., Li, Y., Yin, W., Zu, Y., Li, J., Liu, R., Zhao, F., 2020. Suppressing the radiation-induced corrosion of bismuth nanoparticles for enhanced synergistic cancer radiophototherapy. *ACS Nano* 14 (10), 13016–13029.